J Neurol (2015) 262:2257–2270
DOI 10.1007/s00415-015-7841-1

ORIGINAL COMMUNICATION

Structural hallmarks of amyotrophic lateral sclerosis progression revealed by probabilistic fiber tractography

Robert Steinbach[1] · Kristian Loewe[1,2] · Joern Kaufmann[1] · Judith Machts[1] · Katja Kollewe[3] · Susanne Petri[3] · Reinhard Dengler[3] · Hans-Jochen Heinze[1,4] · Stefan Vielhaber[1] · Mircea Ariel Schoenfeld[1,4,5] · Christian Michael Stoppel[1,4,6]

Received: 5 April 2015 / Revised: 25 June 2015 / Accepted: 29 June 2015 / Published online: 10 July 2015

Abstract Amyotrophic lateral sclerosis (ALS) is a neurodegenerative disease characterized by progressive limb and/or bulbar muscular weakness and atrophy. Although ALS-related alterations of motor and extra-motor neuronal networks have repeatedly been reported, their temporal dynamics during disease progression are not well understood. Recently, we reported a decline of motor system activity and a concurrent increase of hippocampal novelty-evoked modulations across 3 months of ALS progression. To address whether these functional changes are associated with structural ones, the current study employed probabilistic fiber tractography on diffusion tensor imaging (DTI) data using a longitudinal design. Therein, motor network integrity was assessed by DTI-based tracking of the intracranial corticospinal tract, while connectivity estimates of occipito-temporal tracts (between visual and entorhinal, perirhinal or parahippocampal cortices) served to assess structural changes that could be related to the increased novelty-evoked hippocampal activity across time described previously. Complementing these previous functional observations, the current data revealed an ALS-related decrease in corticospinal tract structural connectivity compared to controls, while in contrast, visuo-perirhinal connectivity was relatively increased in the patient group. Importantly, beyond these between-group differences, a rise in the patients' occipito-temporal tract strengths occurred across a 3-month interval, while at the same time no changes in corticospinal tract connectivity were observed. In line with previously identified functional alterations, the dynamics of these structural changes suggest that the affection of motor- and memory-related networks in ALS emerges at distinct disease stages: while motor network degeneration starts primarily during early (supposedly pre-symptomatic) phases, the hippocampal/medial temporal lobe dysfunctions arise at later stages of the disease.

Keywords Amyotrophic lateral sclerosis · Corticospinal tract · Medial temporal lobe · Longitudinal DTI · Probabilistic fiber tractography

✉ Robert Steinbach
robert.steinbach@st.ovgu.de

Christian Michael Stoppel
christian.stoppel@charite.de

[1] Department of Neurology, Otto-von-Guericke-University, Leipziger Str. 44, 39120 Magdeburg, Germany

[2] Department of Knowledge and Language Processing, Otto-von-Guericke-University, Universitätsplatz 2, 39106 Magdeburg, Germany

[3] Department of Neurology, Medical School Hannover, Carl-Neuberg-Str. 1, 30625 Hannover, Germany

[4] Leibniz-Institute for Neurobiology, Brennecke Str. 6, 39118 Magdeburg, Germany

[5] Kliniken Schmieder, Zum Tafelholz 8, 78476 Allensbach, Germany

[6] Present Address: Department of Psychiatry and Psychotherapy, Charité-Universitätsmedizin Berlin, Charitéplatz 1, 10117 Berlin, Germany

Introduction

Amyotrophic lateral sclerosis (ALS) is a neurodegenerative disorder affecting both upper and lower motor neuron functioning and entails a median survival time of only 3 years after symptom onset [1]. While primary motor network degeneration is the pathogenic hallmark of the disease, research during the past decades has revealed

widespread neurodegenerative changes, also encompassing extra-motor sites, predominantly within the frontal lobes [2–7]. These findings led to the conclusion that ALS and fronto-temporal dementia lie on a clinical, pathological, and genetic continuum [8–10].

Beyond this mainly frontal involvement, however, recent research also indicated that memory dysfunctions [11–14] and concordant hippocampal neurodegeneration [3–5, 7, 15, 16] are common during the course of ALS. Based on these reports, we recently conducted a longitudinal functional magnetic resonance imaging (fMRI) study to investigate disease-related changes of hippocampal and motor network functioning during progression of the disease [17]. In this study, we observed a decline of motor-related activity in primary motor cortex within only 3 months of ALS progression, while hippocampal novelty-related activity, in contrast, increased at the same time. These results indicated that hippocampal and motor system lesions emerge at different disease stages: while the decrease in motor activity seems to mirror a breakdown of compensatory mechanisms, the increase in hippocampal activity traditionally has been interpreted in terms of a built-up of compensatory processes following fresh lesions [18–20]. Recent results, however, challenge this notion by demonstrating that pharmacologically induced reduction of such excess hippocampal activity improves cognitive functioning in mild cognitive impairment, thereby suggesting that such increased activations reflect a pathophysiological correlate of the ongoing neurodegeneration rather than a compensatory mechanism [21].

In view of these functional changes, the present study was designed to investigate structural changes complementary to our previous functional results. To this end, probabilistic fiber tractography was performed on diffusion tensor imaging (DTI) data acquired in two scanning sessions separated by a 3-month interval from a comparable ALS patient population. To assess structural integrity of the motor network, DTI-based tracking of the corticospinal tract was conducted between seed regions located in the pontine pyramidal tract and primary motor cortex (Brodmann areas 4a and 4p). Moreover, we also aimed at detecting structural changes related to the previously reported increase in novelty-evoked hippocampal activity. Hence, tractography was conducted between the visual cortex and medial temporal lobe seed regions adjacent to the hippocampal formation, namely the entorhinal, perirhinal, and parahippocampal cortices. These areas were chosen, because previous human and non-human primate studies showed that the information flow between cortical sites (such as the visual cortex), and the hippocampus is relayed via these gateway structures [22–24].

Materials and methods

Subjects

Sixteen patients suffering from sporadic ALS (14 male, mean age 62.1 ± 11.7 years, range 39.4–79.1) and sixteen age- and gender-matched healthy controls (mean age 60.1 ± 12.3 years, range 42–79) were included in this study. All patients met the criteria for probable or definitive ALS as defined by the El Escorial diagnostic criteria [25] and had either limb or bulbar onset. Patients were recruited from the ALS outpatient clinics of the Departments of Neurology at the Medical School Hannover and at the University Hospital Magdeburg. Patients with other neurological conditions, which could affect motor performance or cognition, were excluded from participation. All patients underwent clinical examination on the first day of the study with active follow-up. In order to assess their disease state, the revised ALS Functional Rating Scale score [ALSFRS-R; 26] was obtained (1st session: mean of 41.0 ± 3.6, range of 32–46; 2nd session: mean of 38.2 ± 4.6, range 26–44). The disease duration was defined as time in months since symptom onset until the day of the experiment (1st session: mean of 15.2 ± 10.9 months, range 3–46). Subject demographics and relevant clinical data are shown in Table 1.

Ethical approval for all procedures was obtained prior to the study (Vote number 11/06-75/11, Ethical committee of the Medical Faculty of the Otto-von-Guericke University Magdeburg), and all subjects gave written informed consent before participation. All experimental procedures were performed in accordance with the ethical standards laid down in the 1964 Declaration of Helsinki and its later amendments.

Neuropsychological assessment

For neuropsychological assessment a range of standardized neuropsychological tests were conducted [for detailed description of the employed test battery see 17]. Descriptive analysis of the assessment results (based on the classification scheme introduced by Phukan et al. [13]) showed that 12.5 % of the patients showed selective executive dysfunctions (ALS-Ex, single domain), 19 % had executive dysfunctions paired with (short-term) memory, attention, or visuo-construction deficits (ALS-Ex, multi domain), and another 12.5 % showed impaired attentional performance (non-executive impairment, ALS-NECI). More than half of the enrolled ALS patients (56 %) had no signs of cognitive impairment. Beyond that, none of our 16 patients fulfilled the Neary criteria for fronto-temporal dementia [27]. These results are well in line with previous

Table 1 Socio-demographic and clinical data of the study participants

	Session	ALS patients	Controls	*p* value
Sex	–	14 male, 1 female	14 male, 1 female	1.0
Age	S1	62.1 ± 11.7 years	60.1 ± 12.3 years	0.64
Years of education	S1	14.1 ± 3.1 years	15.6 ± 1.6 years	0.11
Disease duration	S1	15.2 ± 10.9 months	–	–
ALSFRS-R	S1	41.0 ± 3.6	–	–
	S2	38.2 ± 4.6	–	–
Onset type and side	–	5 bulbar, 7 left-hemispheric limb, 4 right-hemispheric limb onset	–	–

The table provides information about gender, age, and years of education for ALS patients and healthy controls. For between-group comparisons two-sample *t* tests were calculated. Table's rightmost column indicates the respective *p* values of these statistical evaluations demonstrating that sex, age, and education did not differ significantly between groups. Below these data, ALSFRS-R scores (depicted separately for each scanning session) as well as the type and side of the disease onset of the patient group are shown. All data (except gender) indicate the group mean and the respective standard deviation

ALSFRS-R revised ALS functional rating scale, *S1* 1st session, *S2* 2nd session

findings from our group, showing that in some patients ALS-related cognitive deficits may include memory dysfunctions, which, however, are distinct from those observed in mild cognitive impairment [28].

DTI data acquisition

DTI data acquisition was conducted on a 3 Tesla Siemens MAGNETOM Trio scanner (Siemens, Erlangen, Germany) with an 8-channel-phased array head coil for signal reception and Syngo VA35 software. For each participant, data were acquired twice, in two sessions separated by a 3-month interval. DTI scans were obtained in an echo planar spin echo sequence [29] using the following parameters: 68 axial slices, TR 8200 ms, TE 89 ms, PAT-modus: GRAPPA (acceleration factor 3, phase oversampling of 25 %), slice thickness 2 mm, *b* value 1000 s/mm^2 (and one additional b0 volume without diffusion gradients applied), acquisition matrix: 128 × 128, and final voxel size: 2 × 2 × 2 mm^3. During each of 4 runs (each with 2 averages and frequency adjustment), one non-diffusion-weighted volume (b0) and 12 diffusion-weighted volumes (non-collinear diffusion gradient directions from Siemens MDDW mode) were acquired.

Processing of DTI data and fiber tracking

All preprocessing steps were carried out using the Functional MRI of the Brain Software Library (FSL v5.0: http://fsl.fmrib.ox.ac.uk/fsl/fslwiki/) [30]. First, DTI data were corrected for eddy-current artifacts and brain extracted. To improve the signal-to-noise ratio, the b0 images from all 4 runs were linearly registered to the first one and subsequently averaged. The parameters from the linear registration were also applied to all 12 diffusion-weighted volumes and gradient directions were aligned accordingly. In order to align the data of both measurements from each subject (separated by the 3-month interval) in an unbiased way, a within-subject template representing the space mid-way between both sessions was created. This template was defined as the average of both b0 images that were linearly registered to the spatial location mid-way between them. Finally, linear and non-linear registrations of the original b0 images of each session to their halfway template were conducted and the resultant parameters were applied to the corresponding gradient images. Tensor decomposition and computation of fractional anisotropy (FA) and mean diffusivity (MD) maps were carried out using FSL's DTIfit tool. To account for differences in the orientation of the resulting images in comparison to the acquired data, subsequent rotation of the corresponding b-vectors was conducted.

Probabilistic fiber tractography was conducted for the intracranial corticospinal tract between the pontine pyramidal tract and the primary motor cortex, and for three tracts between the visual cortex (VC) and medial temporal lobe (MTL) regions known to serve as gateway structures to the hippocampus, i.e., the entorhinal (ERC), perirhinal (PRC), and parahippocampal cortices (PHC). The pontine seed regions of interest (ROIs) for corticospinal tract tractography were defined separately for both brainstem sides on the FMRIB58_FA template in MNI space provided by FSL (http://fsl.fmrib.ox.ac.uk/fsl/fslwiki/FMRIB58_FA). These seed ROIs (manually outlined at bilateral symmetrical locations in one transversal plane, both of which consisted of 11 contiguous voxels) were placed in the medial pons (representing the pontine pyramidal tract) and an additional filter ROI in the posterior limb of the internal capsule (also delineated manually). As seed ROI representing primary motor cortex, cortical areas

4a and 4p [31], as defined in the probabilistic cytoarchitectonic maps provided by the SPM Anatomy Toolbox [32], were thresholded at $p = 0.8$. Similarly, the map of cortical area 17 (thresholded at $p = 0.7$) was used for definition of the visual cortex [33]. The corresponding entorhinal, perirhinal, and parahippocampal ROIs were manually outlined on FSL's T1-weighted volume in MNI space (MNI152_T1) as previously described by Pruessner and colleagues [34]. For the tracts between the visual cortex and the hippocampal gateway regions (entorhinal, perirhinal, and parahippocampal cortices), the entire contralateral hemisphere served as exclusive filter ROI. All ROIs were initially defined in MNI space (using the FMRIB58_FA and MNI152_T1 templates) and subsequently transformed to the subject-specific inter-session space prior to fiber tract reconstruction. To that end, we performed linear and non-linear registration of the subject-specific FA images (in subject-specific halfway inter-session space) to the FMRIB58_FA template in standard MNI space. Then the inversion of the resultant registration parameters was applied to all ROIs. Finally, to retain only white matter voxels, the ROIs were masked with the subject-specific FA image, thresholded at an FA-value of 0.2.

Fiber tract reconstruction was carried out using a probabilistic approach based on a Monte Carlo simulation algorithm that repeatedly searches for probable paths using the diffusion tensor matrix [35]. An estimate of the voxel-specific probability distribution of diffusion directions is used to calculate the probabilities of all allowable propagation steps. During tracking, each step is selected by drawing randomly from this distribution. The number of paths linking two ROIs serves as an estimate of structural connectivity strength between the two. For each seed ROI, tractography was initiated 10,000 times per voxel while counting incident paths for the relevant target ROIs. To exclude implausible paths, anatomically defined filter ROIs were employed. The proportion of plausible paths connecting both ROIs, averaged across tractography directions, served as an index of structural connectivity (CI). More formally, the CI of two ROIs A and B was defined as:

$$\mathrm{CI}(A \leftrightarrow B) = \left[\frac{n(A \rightarrow B)}{n(A \rightarrow brain)} + \frac{n(B \rightarrow A)}{n(B \rightarrow brain)}\right] \Big/ 2 \qquad (1)$$

with $n(A \rightarrow \mathrm{brain})$ being the total number of paths starting from A, and $n(A \rightarrow B)$ being the number of plausible paths starting from A that reach B. The proportion of plausible paths from A to B among all paths starting from A, $n(A \rightarrow B)/n(A \rightarrow \mathrm{brain})$, was used instead of the raw path count, $n(A \rightarrow B)$, in order to account for differences in data quality and inter-individual variability in seed ROI sizes.

Statistical analysis

Statistical analyses were conducted using SPSS 21 (IBM SPSS Statistics, IBM Corporation, Chicago, USA). Significance was assessed by means of repeated measures analysis of variance (RANOVA) with the between-subject factor group (patients vs. controls) and the within-subject factors tract (pons↔primary motor cortex, ERC↔VC, PHC↔VC, PRC↔VC), session (1st vs. 2nd) and hemisphere (left vs. right). If necessary, violations of data sphericity were corrected (Greenhouse–Geisser epsilon) and respective data will be reported with the original degrees of freedom, but with an adjusted level of significance (p values), if exceeding a threshold of $p = 0.05$. In addition, RANOVAs with the between-subject factor group (patients vs. controls) and the within-subject factors session (1st vs. 2nd) and hemisphere (left vs. right) were subsequently conducted separately for each tract. Finally, we aimed to assess correlations between the patients' clinical state and their respective tract strengths. Due to the fact that high correlations of CIs between all occipito-temporal tracts as well as between the left and right corticospinal tract were expected, we first conducted a factor analysis for dimensionality reduction. This analysis revealed significant correlations between CIs of all (bilateral) occipito-temporal (minimum $\rho = 0.570$, all correlations significant with $p < 0.01$) as well as between both corticospinal tracts ($\rho = 0.510$, $p < 0.05$), whereas none of the comparisons across occipito-temporal and corticospinal tract CIs were significantly correlated (maximum $\rho = -0.354$). The factor analysis showed a KMO-Index of 0.692 and a highly significant Bartlett test for sphericity ($X^2 = 114.05$, $p < 0.001$). Two factors with eigenvalues >1 (before rotation: 5.036 and 1.557; after rotation: 5.031 and 1.562) explaining 82.42 % of the total variance (62.95/19.47 % before and 62.89/19.53 % after rotation) were extracted, with a minimum communality for all variables of 0.709. Six (bilateral ERC, PHC and PRC) out of the eight variables loaded on factor 1 (MTL-factor) and two (left and right corticospinal tract) on factor 2 (CST-factor), with the lowest overall factor load on one of both factors of 0.835 before and of 0.838 after rotation. CIs from bilateral corticospinal as well as occipito-temporal tracts clustered and were well separated from each other in the rotated component diagram, each showing high load on only one and low load on the other factor. Finally, after factor extraction, correlations between the patients' ALSFRS-R scores and the extracted MTL-factor data and between their disease duration and the extracted CST-factor values were assessed by calculation of Spearman's rank correlation coefficient ρ.

For fine-grained visualization of pathway-specific tractography results, subject-specific CIs were also computed

at the level of individual voxels. For this aim, the value of each voxel (starting at zero) was incremented by one if it was crossed by a plausible path ($A \rightarrow B$). After this summation procedure, the resultant map was divided by the total number of paths starting from the respective seed ROI [$n(A \rightarrow \text{brain})$]. These single-subject maps were transferred to MNI space by applying the (forward) normalization parameters from the linear and non-linear registrations as already described above and then averaged for both tractography directions. The resultant normalized hit maps were then averaged across sessions and groups. The group-level maps of ALS patients (CI_{ALS}) and controls ($CI_{controls}$) were used to calculate between-group difference maps ($CI_{controls} - CI_{ALS}$) as presented in Fig. 2. In addition, session-level hit maps for the patient group [1st session: CI_{ALS} (S1); 2nd session: CI_{ALS} (S2)] were used to calculate between-session difference maps [CI_{ALS} (S2) − CI_{ALS} (S1)] as shown in Fig. 4.

Results

A RANOVA with the within-subject factors session (1st vs. 2nd), hemisphere and tract, and the between-subject factor group (patients vs. controls) was performed on the participants' CI values. This analysis revealed significant main effects for the factors tract [$F(3,90) = 69.38$, $p < 0.001$] and hemisphere [$F(1,30) = 89.05$, $p < 0.001$], as well as significant tract x group [$F(3,90) = 6.15$, $p = 0.007$], session × group [$F(1,30) = 4.34$, $p = 0.046$], and tract × hemisphere [$F(3,90) = 47.23$, $p < 0.001$] interactions, while the other main effects and interaction terms failed to reach significance. Subsequently, data were analyzed by RANOVAs that were conducted separately for each of the tracts (group mean CI values for each tract—averaged across sessions—are shown in Fig. 1a).

Corticospinal tract structural connectivity and correlation with clinical measures

For the corticospinal tract, ALS patients showed significantly lower CIs than healthy controls [$F(1,30) = 5.21$, $p = 0.03$], while no other main effects or interactions were significant (see leftmost bar graph in Fig. 1a). These data indicate that in ALS patients, fiber strengths within the bilateral corticospinal tract are reduced relative to controls (see Fig. 2a for graphical illustration of the correspondent hit map differences between patients and controls), whereas no further decline in the strength of the corticospinal tracts could be observed across the 3-month interval between sessions.

Beyond this general CI reduction in comparison to controls, we aimed at identifying a potential relationship between the patients' corticospinal tract fiber-strength and their disease state. Since previous studies demonstrated a decline in motor-related activity at later disease stages—and thus on relatively long-time scales compared to the onset of the neurodegeneration [17, 36]—we aimed to assess correlations between the patients' CIs in the bilateral corticospinal tracts and their respective disease durations. Due to the high correlation of CIs between left and right corticospinal as well as across all occipito-temporal tracts, we first conducted a factor analysis on the DTI data for dimensionality reduction (see "Materials and methods" section for detailed description of the factor analysis results). One factor on which CIs of both corticospinal tracts showed high-factor load (CST-factor) was extracted, and the resultant values were then tested for correlation with the patients' disease duration by calculation of Spearman's rank correlation coefficient. By this means, we observed a significant negative correlation between the patients' disease duration and the CST-factor ($\rho = -0.57$, $p = 0.010$), indicating a decline in the patients' pyramidal tract strength with increasing duration of the disease (see Fig. 1b).

Medial temporal lobe structural connectivity and correlation with clinical measures

Beyond the corticospinal tract, we also analyzed CIs for the paths between the visual cortex and medial temporal lobe regions known as gateways to the hippocampus (ERC↔VC, PHC↔VC, PRC↔VC). These analyses revealed a significant main effect of group for the connection between perirhinal and visual cortex [PRC↔VC: $F(1,30) = 5.69$, $p = 0.02$], but not for the other tracts, indicating an increased structural connectivity strength between perirhinal and visual cortex in ALS patients relative to controls (see rightmost bar graph in Fig. 1a, as well as Fig. 2b for the illustration of the correspondent hit map differences between patients and controls). In addition, the analyses also showed a significant interaction between the factors group and session for the tract connecting the perirhinal and visual cortex [$F(1,30) = 5.03$, $p = 0.03$] in terms of an increased structural connectivity between sessions in patients but not in controls, while for the other two occipito-temporal tracts this interaction term just approached significance [PRC↔VC: $F(1,30) = 2.78$, $p = 0.11$; ERC↔VC: $F(1,30) = 3.60$, $p = 0.07$]. For all of the tracts, none of the other main effects or interactions reached or approached significance (see Fig. 3a for session-wise visualization of all three occipito-temporal tracts).

To investigate whether these hippocampal gateway regions might be affected as a whole (since for the tracts between visual and perirhinal/entorhinal cortices the interaction terms just approached the significance

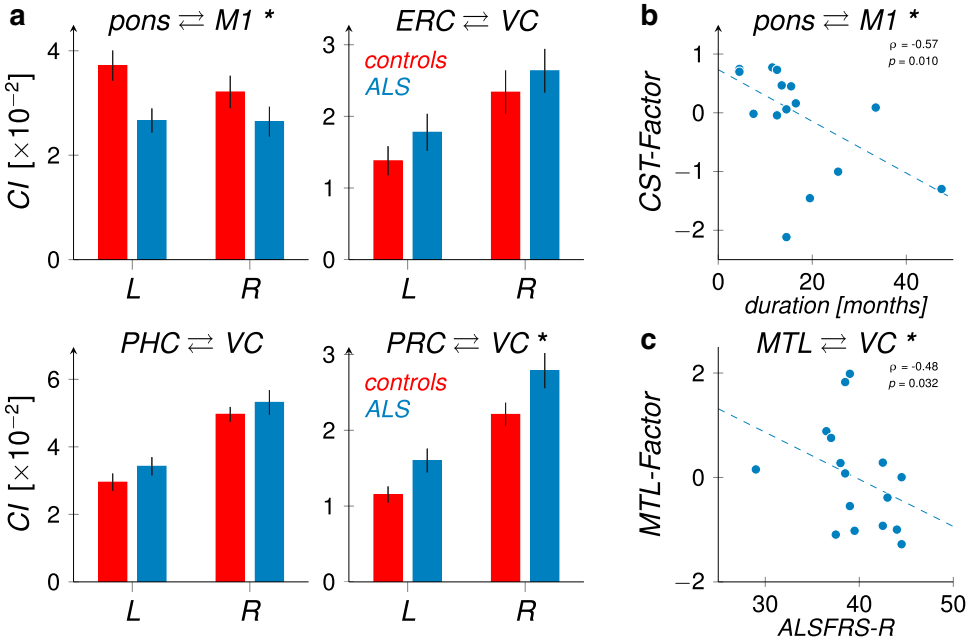

Fig. 1 Group comparison of connectivity indices (CIs) and correlations with clinical measures. **a** Group comparisons of inter-session averaged CIs for all investigated tracts (pons↔M1, ERC↔VC, PHC↔VC and PRC↔VC). Mean CIs for both groups (*red* controls, *blue* ALS patients) are separately depicted for each hemisphere (*L* left, *R* right). *Error bars* represent the standard error of the mean. Within the corticospinal tract, patients showed significantly lower CIs than controls ($p = 0.03$). In contrast, CIs for the tract between perirhinal and visual cortex were relatively increased in the patient group ($p = 0.02$). **b** and **c** Correlations between the patients' clinical measures an their corticospinal (**b**) and occipito-temporal (**c**) tract strengths. Due to the high correlation between CIs across the patients' bilateral corticospinal as well as across all occipito-temporal tracts we performed a dimensionality reduction on these data by factor analysis (see "Materials and methods"). Six (bilateral ERC, PHC and PRC) out of the eight tracts' CIs showed a high-factor load on one (MTL-factor) and the remaining two tracts' CIs (left and right corticospinal tract) on a second factor (CST-factor), with both factors together accounting for 82.42 % of the variance of the data. The resultant CST- and MTL-factor values were subsequently submitted to correlation analyses with the patients' clinical measures (disease durations or ALSFRS-R scores). We observed significant negative correlations between **b** the patients' bilateral corticospinal tract strengths (indexed by the CST-factor) and their disease durations ($\rho = -0.57$, $p = 0.010$) and between their **c** occipito-temporal tract strengths (MTL-factor values) and ALSFRS-R scores ($\rho = -0.48$; $p = 0.032$). *ALSFRS-R* revised ALS functional rating scale, *CI* connectivity index, *CST* corticospinal tract, *M1* primary motor cortex, *ERC* entorhinal cortex, *MTL* medial temporal lobe, *PHC* parahippocampal cortex, *PRC* perirhinal cortex, and *VC* visual cortex. *Asterisks* (*) denote significant effects at a threshold of $p < 0.05$

criterion), we conducted a supplementary analysis (RANOVA with the factors group, hemisphere, and session) on CIs that were averaged across all three occipito-temporal tracts before statistical evaluation [MTL↔VC = (ERC↔VC + PHC↔VC + PRC↔VC)/3; see Fig. 3b]. This analysis revealed a significant session-by-group interaction [$F(1,30) = 4.65$, $p = 0.04$] and a main effect of hemisphere [$F(1,30) = 132.64$, $p < 0.001$], in the absence of other significant main effects or interactions. For a more detailed analysis of the data for the tracts between visual and parahippocampal cortices or between visual cortex and all three medial temporal lobe regions showing a significant session-by-group interaction, additional RANOVAs with the factors hemisphere and session were conducted separately for each of the two groups. For both datasets, these analyses showed a significant main effect of session in patients [higher CI values for the 2nd than for the 1st session; PHC↔VC: $F(1,15) = 5.56$, $p = 0.032$; MTL↔VC: $F(1,15) = 5.37$, $p = 0.035$], but not in controls [PHC↔VC: $F(1,15) = 0.57$, $p = 0.46$; MTL↔VC: $F(1,15) = 0.29$, $p = 0.60$]. In summary, these data show that CIs in the patients' occipito-temporal tracts increased within only 3 months of ALS progression (for visualization of the patients' respective hit map differences across session for the tract between parahippocampal and visual cortex see Fig. 4), beyond an already existent increase in the patients' CIs within the tract between perirhinal and visual cortex relative to controls (see Fig. 2b).

As for the corticospinal tract, we aimed to investigate if disease-related changes in connectivity strengths between the hippocampal gateway regions in the medial temporal lobe and the visual cortex correlated with the patients' clinical state. Due to the fact that an involvement of the hippocampus has been suggested to arise at much later disease stages than the motor system lesions [17] and might thus be less related to the actual duration of the disease, we instead aimed to assess putative correlations between the

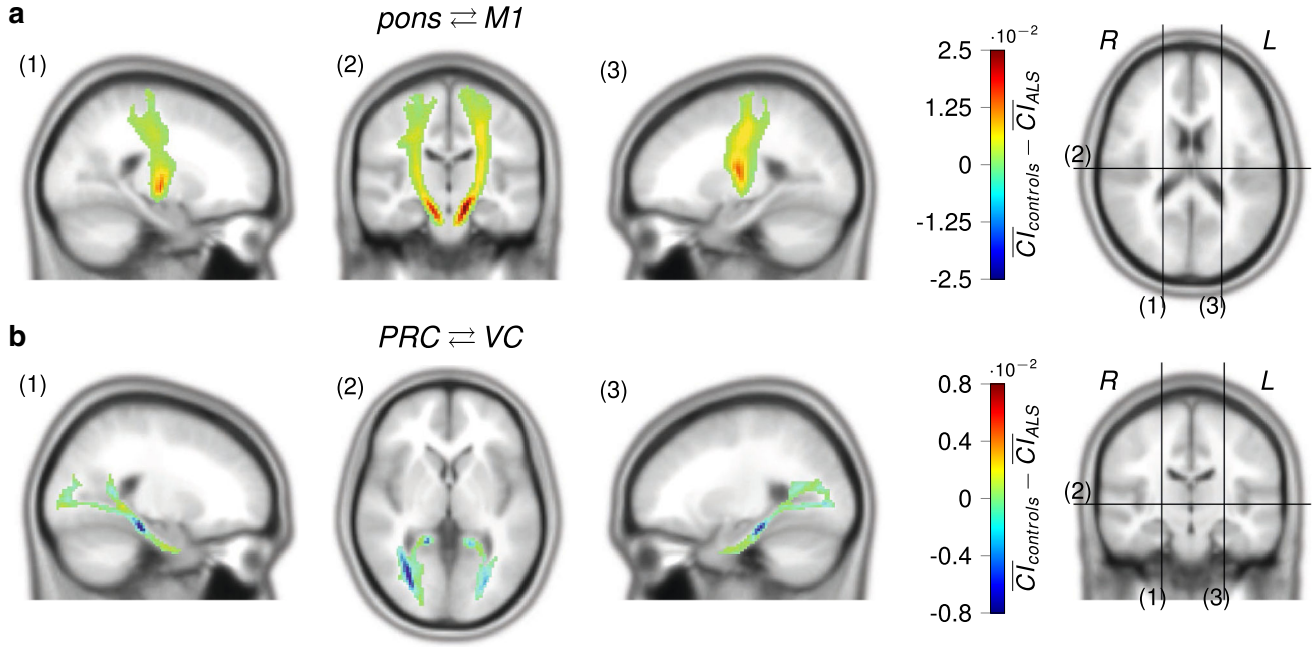

Fig. 2 Visualization of hit map differences between patients and controls for the bilateral corticospinal (pons↔M1) and the bilateral PRC↔VC tract. The figure displays the relative hit map difference values between patients and controls for **a** the bilateral corticospinal and **b** the bilateral PRC↔VC tract (see "Materials and methods" for description of the calculation procedure for the hit map difference values). Warm colors (*yellow* to *red*) indicate voxels with relatively higher hit map values in controls, while cold colors (*cyan* to *dark blue*) represent voxels showing relatively increased hit map values in the patient group. Numbers above brain slices (1–3) refer to the respective plane as depicted in the rightmost brain images. Note that patients displayed lower hit map values in the bilateral corticospinal tract compared to controls, while the opposed pattern could be observed in the PRC↔VC tract (higher hit map values in patients than in controls). *L* left hemisphere, *M1* primary motor cortex, *PRC* perirhinal cortex, *R* right hemisphere, *VC* visual cortex

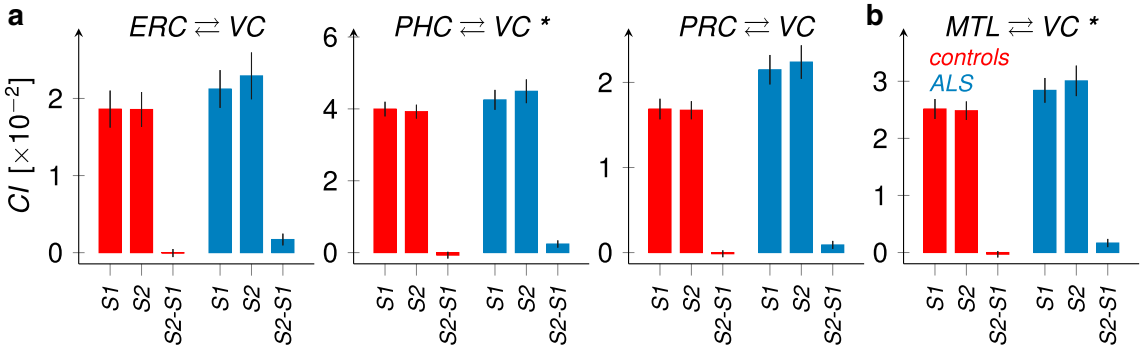

Fig. 3 Session-wise visualization of CIs for the occipito-temporal tracts (ERC↔VC, PHC↔VC and PRC↔VC) and their mean (MTL↔VC). For both groups (*red* controls, *blue* ALS patients) session-wise CI values and their inter-session differences are shown (*S1* 1st session, *S2* 2nd session; *S2-S1* = 2nd−1st session). **a** Separate visualization of group and session-wise CIs for each of the three occipito-temporal tracts: ERC↔VC, PHC↔VC and PRC↔VC. *Error bars* represent the standard error of the mean. CIs of the PHC↔VC tract showed a significant group × session interaction [$F(1,30) = 5.03$, $p = 0.03$], while this interaction term only approached significance for the ERC↔VC and PRC↔VC tracts [PRC↔VC: $F(1,30) = 2.78$, $p = 0.11$; ERC↔VC: $F(1,30) = 3.60$, $p = 0.07$]. Note that the (almost) significant interactions are due an increase of the CIs from the 1st to the 2nd session in patients, which was absent in controls. **b** Mean CIs across all three occipito-temporal tracts (MTL↔VC). *Bars* represent mean CI values averaged across all three occipito-temporal tracts: MTL↔VC = (ERC↔VC + PHC↔VC + PRC↔VC)/3. Analysis of these mean occipito-temporal CIs (MTL↔VC) revealed a significant group-by-session interaction [$F(1,30) = 4.65$, $p = 0.04$] due to a rise in the patients' CIs from the 1st to the 2nd measurement, which was absent in controls. *CI* connectivity index, *M1* primary motor cortex, *ERC* entorhinal cortex, *PHC* parahippocampal cortex, *PRC* perirhinal cortex, *VC* visual cortex, and *MTL* medial temporal lobe. *Asterisks* (*) denote significant effects at a threshold of $p < 0.05$

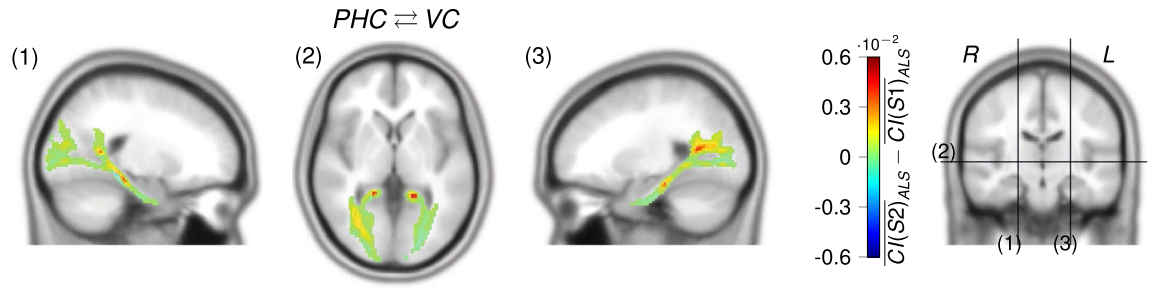

Fig. 4 Visualization of hit map differences between sessions for the bilateral PHC↔VC tract in ALS patients. The figure displays the patients' relative hit map difference values between sessions for the bilateral PHC↔VC tract (see "Materials and methods" for description of the calculation procedure for the inter-session difference values). Warm colors (*yellow* to *red*) indicate voxels with relatively higher hit map values in the 2nd session, while cold colors (*cyan* to *dark blue*) represent voxels showing relatively increased hit map values in the 1st session. Numbers above brain slices (1–3) refer to the respective plane as depicted in the rightmost brain image. Note that in ALS patients, parts of the bilateral PHC↔VC tract show an increase of hit map values during the 3-month interval (higher hit map values during the 2nd than during the 1st session). *L* left hemisphere, *PHC* parahippocampal cortex, *R* right hemisphere, *S1* 1st session, *S2* 2nd session, and *VC* visual cortex

patients' ALSFRS-R scores and their occipito-temporal tract strengths. The rationale was that the ALSFRS-R is a compound score (including ratings beyond a mere affection of the motor system), for some of whose sub-scales an ALS-related decline has been shown to arise at later stages of the disease [for a similar line of reasoning concerning correlations with clinical measures see 3]. As for the corticospinal tract data, correlations between CIs of the occipito-temporal tracts and the patients' ALSFRS-R scores were not directly calculated due to high correlations across CIs of all occipito-temporal tracts. Instead we employed the extracted MTL-factor from the factor analysis, on which CIs from all occipito-temporal showed a high-factor load. Therein we observed a significant inverse correlation between the patients' ALSFRS-R scores and the extracted MTL-factor values ($\rho = -0.48$; $p = 0.032$). These data indicate that a rise in the occipito-temporal tracts' CIs occurs with increasing disability of the patients (see Fig. 1c), providing additional evidence for the notion that changes in structural connectivity of these projecting tracts toward the medial temporal lobe might in fact emerge at later disease stages than those within the corticospinal tract.

Beyond the significant effects reported so far, we also observed a main effect of hemisphere for all three occipito-temporal tracts [PRC↔VC: $F(1,30) = 117.28$, $p < 0.001$; ERC↔VC: $F(1,30) = 47.02$, $p < 0.001$; PHC↔VC: $F(1,30) = 117.50$, $p < 0.001$; see also the results from the mean medial temporal lobe data reported above], in the absence of significant interactions for this within-subject factor. These data show, that all investigated occipito-temporal tracts displayed higher CIs within the right compared to the left hemisphere, irrespective of the particular scanning session or group membership of the subjects (see Fig. 1a).

Discussion

Complementing our previous fMRI findings [17], the current results revealed an ALS-related decrease in corticospinal tract structural connectivity compared to healthy individuals, while the connectivity strength between perirhinal and visual cortex, in contrast, was higher within the patient group. Importantly, beyond these differences in comparison to healthy controls we also observed an increase in the patients' occipito-temporal tract strengths across the 3-month interval between measurements. These results support the view that in ALS, lesions across different neural networks (as e.g., the occipito-temporal and the motor system) develop at distinct stages of the disease. In this regard, our findings provide additional evidence for a stepwise progression of ALS-related brain changes across different neural systems and suggest that the emergence and/or detectability of structural (and functional) alterations might be closely linked to distinct periods of the disease.

Alterations of corticospinal tract structural connectivity in ALS

In the current study, we observed a reduced structural connectivity of the corticospinal tract in ALS patients in comparison to healthy individuals. Beyond these changes, however, our data did not reveal further longitudinal (within-subject) structural connectivity changes in the patients' corticospinal tract across the 3-month interval between measurements. Taken together, these data are in good agreement with the majority of previous work concerning motor network integrity in ALS. Multiple in vivo investigations—using different MR imaging approaches—consistently reported alterations (e.g., of MR signal

intensities, gray and white matter volumes, diffusivity measures, as well as the magnitude of functional activations) of the precentral gyrus and the adjacent corticospinal tract in ALS [for review see 2,10,37]. While these data have initially been interpreted to reflect the ongoing motor system degeneration, this notion has been questioned in view of more recent findings. First, it has been shown that neurodegenerative processes occur long before clinical signs become apparent [38, 39] and, consistently, a decrease of corticospinal tract fractional anisotropy in presymptomatic carriers of the pathogenic SOD1 mutation has been observed [40]. Secondly, multiple fMRI investigations observed increased activations of motor and premotor regions in ALS [e.g., 41–43], which initially have been explained in terms of a functional adaptation or compensatory recruitment as a result of motor system degeneration. More recently, however, it has been shown that such hyperactivity might be rather prototypical for early-stage lesions [17–20], whereas this hyperactivity gradually disappears with progression of the ALS-related neurodegeneration [17, 44]. Beyond the interpretation of this hyperactivity in terms of a compensatory resource recruitment, recent evidence suggests it to reflect a pathophysiological correlate of the ongoing neurodegeneration by showing that a pharmacologically induced reduction of such excess (hippocampal) activity may improve cognitive functioning in mild cognitive impairment [21]. Although the underlying pathophysiological mechanisms and the functional implications of this hyperexcitability seen during early-stage neurodegeneration are not yet understood, the longitudinal pattern of an initial increase followed by a subsequent decline in brain activity has repeatedly been demonstrated and also seems to be valid for the course of the progression of ALS.

Finally, the majority of longitudinal studies on structural connectivity changes in ALS—though only a handful have been conducted to date—found either no or only minor progressive changes in the corticospinal tract with ongoing clinical progression of the disease [3, 36, 45–50]. Altogether, these findings suggest that the core corticospinal tract degeneration emerges during early ALS stages (most likely even before clinical signs become apparent), but they do not seem to be subject of major changes during the later course of the disease [for a similar line of reasoning see 3]. Our current results are fully compatible with this view, in that we found a decreased structural connectivity of the corticospinal tract in ALS patients, while they showed no evidence for ongoing corticospinal tract degeneration across the 3-month interval between measurements. Accordingly, we observed a correlation between the structural integrity of our patients' corticospinal tracts (indexed by the compound CST-factor data from our factor analysis) and the patients' disease duration, corroborating the view that changes in corticospinal tract integrity occur on a long-time scale (at least much longer than 3 months), while at later stages the motor network changes are predominantly functional in nature [17, 43].

Alterations in medial temporal lobe structural connectivity in ALS

In contrast to the decreased CIs in the patients' corticospinal tract, we observed an opposed pattern for the structural connections between the visual cortex and medial temporal lobe regions adjacent to the hippocampal formation. On the one hand, our data revealed significantly higher CIs in the tract between perirhinal and visual cortices of the patients relative to controls, while on the other hand our data showed that the patients' CIs between parahippocampal and visual cortex (but also the mean CIs of all three investigated occipito-temporal tracts) increased across the 3-month interval. At first glance, such an enhanced structural connectivity—as a result of a progressive neurodegenerative disease like ALS—seems to be counterintuitive. Nevertheless, our results fit well with analogous findings reported recently for hyper-acute stages of stroke or early-stage neurodegenerative diseases.

While, to our knowledge, no prior study observed signs for an increased structural connectivity in neurodegenerative diseases or brain injury by means of fiber tracking, multiple investigations reported comparable changes of scalar DTI measures like fractional anisotropy (FA) or mean diffusivity (MD). As such, an increased FA, with a concomitant decrease of MD, has repeatedly been reported to occur during hyper-acute stages of stroke [51–53] or semi-acute stages of mild traumatic brain injury [54–57]. Such FA increases have been linked to acute microstructural neurodegeneration in the absence of significant damage to the gross structural coherence of the underlying fiber architecture and considered to reflect an initial neuronal damage [followed by a phase of inverse alterations, i.e., decreased FA and increased MD; see 58, 59, 60]. Therein, several (sub-) cellular processes have been linked to such changed DTI measures. For one, the acute increase in FA has been associated with cytotoxic edema and a subsequent increase in the tortuosity of the extracellular space [61], a shift of water from the extracellular to the more restricted intracellular space and resultant axonal swelling [62–64], as well as a reduction of water inside the myelin sheath [65].

Other—though in face of our current results rather unlikely—causal mechanisms for an increased FA (as e.g., seen in studies on normal aging, mild cognitive impairment or stroke) are a seemingly increased structural integrity caused by a loss of crossing fibers [66–71], a reduction of diffusion barriers due to changes of the neuronal micro-

organization such as decreased dendritic arborization [72, 73] or a selective degeneration of local inhibitory interneurons.

Taken together, these mechanistic accounts, in concert with our previous functional results, suggest that the patients' increased occipito-temporal CIs observed in the present study are the macroscopic representation of microcellular alterations during early-stage neurodegeneration.

Temporal evolution of (structural and functional) brain changes in ALS

Apart from these considerations concerning the pathophysiological foundations of the structural changes, our current results [in conjunction with our previous fMRI findings; 17] also need to be evaluated in light of their putative temporal evolution with respect to ALS disease progression. With this said, it is important to note that we observed opposed patterns of functional and structural changes within the hippocampal (increased structural connectivity and increased fMRI activations) and the motor system (decreased structural connectivity and initially enlarged but subsequently declining fMRI activity). As already delineated in the first section of the discussion, the motor network changes seem to constitute late-stage neurodegenerative alterations: while during early stages the hemodynamic activations increase, they show a decline with further progression of the disease. Concordantly, our DTI results revealed a decreased corticospinal tract structural integrity in ALS patients relative to controls, indicative of a rather late-stage neurodegenerative process. This view is further supported by the fact that no further longitudinal reduction in the patients' CIs could be detected across the 3-month study-interval. Such steady-state structural integrity of the corticospinal tract during ongoing clinical ALS progression has repeatedly been described and was interpreted as a sign of late-stage neurodegeneration [3, 36, 45–48].

Opposed to these motor system alterations, the patients' increased CIs within the tracts between medial temporal and visual cortices (relative to controls or within-subjects across the 3-month interval) seem to reflect structural changes as a result of rather early hippocampal lesions. As outlined in the previous paragraph, the supposedly increased structural connectivity (i.e., increased CIs) seems to mirror acute neurodegenerative processes in terms of microstructural damage in the absence of coarse changes to the general fiber architecture. In line with this, we observed a correlation between the patients' occipito-temporal tract strengths (by means of the compound MTL-factor data from our factor analysis) and their ALSFRS-R scores (for most patients these were still in a range of a minor impairment), for which an ALS-related decline has been shown to arise mainly at late disease stages [for a similar line of reasoning see 3]. Taken together, these data suggest that the non-invasively detectable (structural and functional) neurodegenerative changes in ALS might follow a non-linear course: while fresh lesions result in an increased functional activity and a supposedly increased structural connectivity (as detected in the medial temporal lobe of our patients), both subsequently seem to decline (reflected by the functional decline of motor activity in our previous study), finally resulting in impaired functionality and diminished structural integrity in late-stage ALS (as seen in our current and most previous investigations on motor network integrity in ALS).

Limitations and future directions

Concerning the variety of putative causal microstructural changes discussed above (see subsection "Alterations in medial temporal lobe structural connectivity in ALS"), our current design and employed methodology are not suited to prove, which of them might be the most likely cause for the increased CIs we observed by means of probabilistic fiber tractography in the occipito-temporal tracts of our patients. Beyond that, the data acquisition methodology employed during the current study (i.e., an acquisition of only 12 diffusion gradient directions) has a limited capacity in obtaining differential directionality information in order to detect microstructural changes of smaller fiber bundles, which are especially true for regions containing crossing fibers [74, 75], although major differences in DTI parameters were shown to be detectable with comparable data [2, 50, 76]. In light of this, but also with regard to earlier investigations on structural connectivity in neurodegenerative diseases, the development and application of more sensitive diffusion imaging techniques, such as high angular resolution diffusion imaging and neurite orientation dispersion and density imaging, is mandatory [77, 78].

In addition, as our patients were only scanned twice within 3 months and pre-symptomatic mutation carriers were not included in our study, the factual temporal evolution of structural and functional changes remains elusive. Employing novel imaging methodology in longitudinal studies, beginning with pre-symptomatic carriers and systematic follow-up along the progression of the diseases, is critical to advance our understanding of the origins and the progression mechanisms, as well as to allow for valid predictions concerning the development and courses of these disorders. The importance of such longitudinal designs becomes even more compelling, given that a growing number of studies could demonstrate that the structural and functional alterations during progressive neurodegeneration seem to follow a non-linear course, with

distinct patterns arising during different stages of the diseases [3, 17, 36, 45–48].

Conclusions

The present longitudinal investigation revealed opposed ALS-related structural alterations in the corticospinal and occipito-temporal tracts by means of probabilistic fiber tractography, thereby complementing our previous structural and fMRI results [17]. Our findings once more indicate that ALS is a multisystem disorder, in which the hippocampus and its' structural connections also are affected. In contrast to our previous functional results, however, we did not observe dynamic motor system changes across the 3-month interval, while structural connectivity between the visual cortex and hippocampal gateway regions in the medial temporal lobe appeared to increase at the same time. The dynamics of these structural changes thus again suggest that the affection of motor- and memory-related networks in ALS emerges at different stages of the disease. While the motor system lesions develop rather early (supposedly during pre-symptomatic stages), the hippocampal/medial temporal lobe dysfunctions arise much later in the course of the disease. Insights into such progression-related dynamics across different functional systems (motor, memory, etc.) is essential for our understanding of the origin and the progression of ALS, thus highlighting the importance of further longitudinal investigations to advance our knowledge of the biological grounds of this debilitating disease.

Acknowledgments This work was supported by the Deutsche Forschungsgemeinschaft (Scho 1217/1-2 and SFB 779 - A1 to M.A.S.).

Conflicts of interest The authors declare that they have no conflict of interest.

References

1. Hardiman O, van den Berg LH, Kiernan MC (2011) Clinical diagnosis and management of amyotrophic lateral sclerosis. Nature Rev Neurol 7(11):639–649. doi:10.1038/nrneurol.2011.153
2. Agosta F, Chio A, Cosottini M, De Stefano N, Falini A, Mascalchi M, Rocca MA, Silani V, Tedeschi G, Filippi M (2010) The present and the future of neuroimaging in amyotrophic lateral sclerosis. AJNR Am J Neuroradiol 31(10):1769–1777. doi:10.3174/ajnr.A2043
3. Menke RA, Korner S, Filippini N, Douaud G, Knight S, Talbot K, Turner MR (2014) Widespread grey matter pathology dominates the longitudinal cerebral MRI and clinical landscape of amyotrophic lateral sclerosis. Brain J Neurol 137(Pt 9):2546–2555. doi:10.1093/brain/awu162
4. Neumann M, Sampathu DM, Kwong LK, Truax AC, Micsenyi MC, Chou TT, Bruce J, Schuck T, Grossman M, Clark CM, McCluskey LF, Miller BL, Masliah E, Mackenzie IR, Feldman H, Feiden W, Kretzschmar HA, Trojanowski JQ, Lee VM (2006) Ubiquitinated TDP-43 in frontotemporal lobar degeneration and amyotrophic lateral sclerosis. Science 314(5796):130–133. doi:10.1126/science.1134108
5. Takeda T, Uchihara T, Arai N, Mizutani T, Iwata M (2009) Progression of hippocampal degeneration in amyotrophic lateral sclerosis with or without memory impairment: distinction from Alzheimer disease. Acta Neuropathol 117(1):35–44. doi:10.1007/s00401-008-0447-2
6. van der Graaff MM, Sage CA, Caan MW, Akkerman EM, Lavini C, Majoie CB, Nederveen AJ, Zwinderman AH, Vos F, Brugman F, van den Berg LH, de Rijk MC, van Doorn PA, Van Hecke W, Peeters RR, Robberecht W, Sunaert S, de Visser M (2011) Upper and extra-motoneuron involvement in early motoneuron disease: a diffusion tensor imaging study. Brain J Neurol 134(Pt 4):1211–1228. doi:10.1093/brain/awr016
7. Wightman G, Anderson VE, Martin J, Swash M, Anderton BH, Neary D, Mann D, Luthert P, Leigh PN (1992) Hippocampal and neocortical ubiquitin-immunoreactive inclusions in amyotrophic lateral sclerosis with dementia. Neurosci Lett 139(2):269–274
8. Lomen-Hoerth C, Anderson T, Miller B (2002) The overlap of amyotrophic lateral sclerosis and frontotemporal dementia. Neurology 59(7):1077–1079
9. Rademakers R, Neumann M, Mackenzie IR (2012) Advances in understanding the molecular basis of frontotemporal dementia. Nature Rev Neurol 8(8):423–434. doi:10.1038/nrneurol.2012.117
10. Tsermentseli S, Leigh PN, Goldstein LH (2012) The anatomy of cognitive impairment in amyotrophic lateral sclerosis: more than frontal lobe dysfunction. Cortex 48(2):166–182. doi:10.1016/j.cortex.2011.02.004
11. Hammer A, Vielhaber S, Rodriguez-Fornells A, Mohammadi B, Munte TF (2011) A neurophysiological analysis of working memory in amyotrophic lateral sclerosis. Brain Res 1421:90–99. doi:10.1016/j.brainres.2011.09.010
12. Mantovan MC, Baggio L, Dalla Barba G, Smith P, Pegoraro E, Soraru G, Bonometto P, Angelini C (2003) Memory deficits and retrieval processes in ALS. Eur J Neurol 10(3):221–227. doi:607ii
13. Phukan J, Elamin M, Bede P, Jordan N, Gallagher L, Byrne S, Lynch C, Pender N, Hardiman O (2012) The syndrome of cognitive impairment in amyotrophic lateral sclerosis: a population-based study. J Neurol Neurosurg Psychiatry 83(1):102–108. doi:10.1136/jnnp-2011-300188
14. Raaphorst J, de Visser M, Linssen WH, de Haan RJ, Schmand B (2010) The cognitive profile of amyotrophic lateral sclerosis: a meta-analysis. Amyotroph Lateral Scler 11(1–2):27–37. doi:10.3109/17482960802645008
15. Anderson VE, Cairns NJ, Leigh PN (1995) Involvement of the amygdala, dentate and hippocampus in motor neuron disease. J Neurol Sci 129(Suppl):75–78. doi:0022510X9500069E
16. Takeda T, Uchihara T, Mochizuki Y, Mizutani T, Iwata M (2007) Memory deficits in amyotrophic lateral sclerosis patients with dementia and degeneration of the perforant pathway A clinicopathological study. J Neurol Sci 260(1–2):225–230. doi:10.1016/j.jns.2007.05.010
17. Stoppel CM, Vielhaber S, Eckart C, Machts J, Kaufmann J, Heinze HJ, Kollewe K, Petri S, Dengler R, Hopf JM, Schoenfeld MA (2014) Structural and functional hallmarks of amyotrophic lateral sclerosis progression in motor- and memory-related brain regions. NeuroImage Clin 5:277–290. doi:10.1016/j.nicl.2014.07.007
18. Bookheimer SY, Strojwas MH, Cohen MS, Saunders AM, Pericak-Vance MA, Mazziotta JC, Small GW (2000) Patterns of brain activation in people at risk for Alzheimer's disease. N Engl J Med 343(7):450–456. doi:10.1056/NEJM200008173430701

19. Dickerson BC, Sperling RA (2008) Functional abnormalities of the medial temporal lobe memory system in mild cognitive impairment and Alzheimer's disease: insights from functional MRI studies. Neuropsychologia 46(6):1624–1635. doi:10.1016/j.neuropsychologia.2007.11.030
20. Woodard JL, Seidenberg M, Nielson KA, Antuono P, Guidotti L, Durgerian S, Zhang Q, Lancaster M, Hantke N, Butts A, Rao SM (2009) Semantic memory activation in amnestic mild cognitive impairment. Brain 132(Pt 8):2068–2078. doi:10.1093/brain/awp157
21. Bakker A, Krauss GL, Albert MS, Speck CL, Jones LR, Stark CE, Yassa MA, Bassett SS, Shelton AL, Gallagher M (2012) Reduction of hippocampal hyperactivity improves cognition in amnestic mild cognitive impairment. Neuron 74(3):467–474. doi:10.1016/j.neuron.2012.03.023
22. Lavenex P, Amaral DG (2000) Hippocampal-neocortical interaction: a hierarchy of associativity. Hippocampus 10(4):420–430. doi:10.1002/1098-1063(2000)10:4<420:AID-HIPO8>3.0.CO;2-5
23. Powell HW, Guye M, Parker GJ, Symms MR, Boulby P, Koepp MJ, Barker GJ, Duncan JS (2004) Noninvasive in vivo demonstration of the connections of the human parahippocampal gyrus. NeuroImage 22(2):740–747. doi:10.1016/j.neuroimage.2004.01.011
24. Squire LR (1992) Declarative and nondeclarative memory: multiple brain systems supporting learning and memory. J Cogn Neurosci 4(3):232–243. doi:10.1162/jocn.1992.4.3.232
25. Brooks BR, Miller RG, Swash M, Munsat TL, World Federation of Neurology Research Group on Motor Neuron D (2000) El Escorial revisited: revised criteria for the diagnosis of amyotrophic lateral sclerosis. Amyotroph Lateral Scler Other Motor Neuron Disord 1(5):293–299
26. Cedarbaum JM, Stambler N, Malta E, Fuller C, Hilt D, Thurmond B, Nakanishi A (1999) The ALSFRS-R: a revised ALS functional rating scale that incorporates assessments of respiratory function. BDNF ALS Study Group (Phase III). J Neurol Sci 169(1–2):13–21. doi:S0022510X99002105
27. Neary D, Snowden JS, Gustafson L, Passant U, Stuss D, Black S, Freedman M, Kertesz A, Robert PH, Albert M, Boone K, Miller BL, Cummings J, Benson DF (1998) Frontotemporal lobar degeneration: a consensus on clinical diagnostic criteria. Neurology 51(6):1546–1554
28. Machts J, Bittner V, Kasper E, Schuster C, Prudlo J, Abdulla S, Kollewe K, Petri S, Dengler R, Heinze HJ, Vielhaber S, Schoenfeld MA, Bittner DM (2014) Memory deficits in amyotrophic lateral sclerosis are not exclusively caused by executive dysfunction: a comparative neuropsychological study of amnestic mild cognitive impairment. BMC Neurosci 15:83. doi:10.1186/1471-2202-15-83
29. Reese TG, Heid O, Weisskoff RM, Wedeen VJ (2003) Reduction of eddy-current-induced distortion in diffusion MRI using a twice-refocused spin echo. Magnetic Reson Med 49(1):177–182. doi:10.1002/mrm.10308
30. Jenkinson M, Beckmann CF, Behrens TE, Woolrich MW, Smith SM (2012) Fsl. NeuroImage 62(2):782–790. doi:10.1016/j.neuroimage.2011.09.015
31. Geyer S, Ledberg A, Schleicher A, Kinomura S, Schormann T, Burgel U, Klingberg T, Larsson J, Zilles K, Roland PE (1996) Two different areas within the primary motor cortex of man. Nature 382(6594):805–807. doi:10.1038/382805a0
32. Eickhoff SB, Stephan KE, Mohlberg H, Grefkes C, Fink GR, Amunts K, Zilles K (2005) A new SPM toolbox for combining probabilistic cytoarchitectonic maps and functional imaging data. NeuroImage 25(4):1325–1335. doi:10.1016/j.neuroimage.2004.12.034
33. Amunts K, Malikovic A, Mohlberg H, Schormann T, Zilles K (2000) Brodmann's areas 17 and 18 brought into stereotaxic space-where and how variable? NeuroImage 11(1):66–84. doi:10.1006/nimg.1999.0516
34. Pruessner JC, Kohler S, Crane J, Pruessner M, Lord C, Byrne A, Kabani N, Collins DL, Evans AC (2002) Volumetry of temporopolar, perirhinal, entorhinal and parahippocampal cortex from high-resolution MR images: considering the variability of the collateral sulcus. Cereb Cortex 12(12):1342–1353
35. Bodammer NC, Kaufmann J, Kanowski M, Tempelmann C (2009) Monte Carlo-based diffusion tensor tractography with a geometrically corrected voxel-centre connecting method. Phys Med Biol 54(4):1009–1033. doi:10.1088/0031-9155/54/4/013
36. Agosta F, Gorno-Tempini ML, Pagani E, Sala S, Caputo D, Perini M, Bartolomei I, Frugulietti ME, Filippi M (2009) Longitudinal assessment of grey matter contraction in amyotrophic lateral sclerosis: a tensor based morphometry study. Amyotroph Lateral Scler 10(3):168–174. doi:10.1080/17482960802603841
37. Foerster BR, Welsh RC, Feldman EL (2013) 25 years of neuroimaging in amyotrophic lateral sclerosis. Nature Rev Neurol 9(9):513–524. doi:10.1038/nrneurol.2013.153
38. Aggarwal A, Nicholson G (2002) Detection of preclinical motor neurone loss in SOD1 mutation carriers using motor unit number estimation. J Neurol Neurosurg Psychiatry 73(2):199–201
39. de Carvalho M, Swash M (2006) The onset of amyotrophic lateral sclerosis. J Neurol Neurosurg Psychiatry 77(3):388–389. doi:10.1136/jnnp.2005.073031
40. Ng MC, Ho JT, Ho SL, Lee R, Li G, Cheng TS, Song YQ, Ho PW, Fong GC, Mak W, Chan KH, Li LS, Luk KD, Hu Y, Ramsden DB, Leong LL (2008) Abnormal diffusion tensor in nonsymptomatic familial amyotrophic lateral sclerosis with a causative superoxide dismutase 1 mutation. J Magn Reson Imaging 27(1):8–13. doi:10.1002/jmri.21217
41. Kew JJ, Leigh PN, Playford ED, Passingham RE, Goldstein LH, Frackowiak RS, Brooks DJ (1993) Cortical function in amyotrophic lateral sclerosis. A positron emission tomography study. Brain 116(Pt 3):655–680
42. Kollewe K, Munte TF, Samii A, Dengler R, Petri S, Mohammadi B (2011) Patterns of cortical activity differ in ALS patients with limb and/or bulbar involvement depending on motor tasks. J Neurol 258(5):804–810. doi:10.1007/s00415-010-5842-7
43. Schoenfeld MA, Tempelmann C, Gaul C, Kuhnel GR, Duzel E, Hopf JM, Feistner H, Zierz S, Heinze HJ, Vielhaber S (2005) Functional motor compensation in amyotrophic lateral sclerosis. J Neurol 252(8):944–952. doi:10.1007/s00415-005-0787-y
44. Mohammadi B, Kollewe K, Samii A, Dengler R, Munte TF (2011) Functional neuroimaging at different disease stages reveals distinct phases of neuroplastic changes in amyotrophic lateral sclerosis. Hum Brain Mapp 32(5):750–758. doi:10.1002/hbm.21064
45. Blain CR, Williams VC, Johnston C, Stanton BR, Ganesalingam J, Jarosz JM, Jones DK, Barker GJ, Williams SC, Leigh NP, Simmons A (2007) A longitudinal study of diffusion tensor MRI in ALS. Amyotroph Lateral Scler 8(6):348–355. doi:10.1080/17482960701548139
46. Kwan JY, Meoded A, Danielian LE, Wu T, Floeter MK (2012) Structural imaging differences and longitudinal changes in primary lateral sclerosis and amyotrophic lateral sclerosis. NeuroImage Clin 2:151–160. doi:10.1016/j.nicl.2012.12.003
47. Menke RA, Abraham I, Thiel CS, Filippini N, Knight S, Talbot K, Turner MR (2012) Fractional anisotropy in the posterior limb of the internal capsule and prognosis in amyotrophic lateral sclerosis. Arch Neurol 69(11):1493–1499. doi:10.1001/archneurol.2012.1122

48. Mitsumoto H, Ulug AM, Pullman SL, Gooch CL, Chan S, Tang MX, Mao X, Hays AP, Floyd AG, Battista V, Montes J, Hayes S, Dashnaw S, Kaufmann P, Gordon PH, Hirsch J, Levin B, Rowland LP, Shungu DC (2007) Quantitative objective markers for upper and lower motor neuron dysfunction in ALS. Neurology 68(17):1402–1410. doi:10.1212/01.wnl.0000260065.57832.87
49. Keil C, Prell T, Peschel T, Hartung V, Dengler R, Grosskreutz J (2012) Longitudinal diffusion tensor imaging in amyotrophic lateral sclerosis. BMC Neurosci 13:141. doi:10.1186/1471-2202-13-141
50. Zhang Y, Schuff N, Woolley SC, Chiang GC, Boreta L, Laxamana J, Katz JS, Weiner MW (2011) Progression of white matter degeneration in amyotrophic lateral sclerosis: a diffusion tensor imaging study. Amyotroph Lateral Scler 12(6):421–429. doi:10.3109/17482968.2011.593036
51. Bhagat YA, Hussain MS, Stobbe RW, Butcher KS, Emery DJ, Shuaib A, Siddiqui MM, Maheshwari P, Al-Hussain F, Beaulieu C (2008) Elevations of diffusion anisotropy are associated with hyper-acute stroke: a serial imaging study. Magn Reson Imaging 26(5):683–693. doi:10.1016/j.mri.2008.01.015
52. Herve D, Molko N, Pappata S, Buffon F, LeBihan D, Bousser MG, Chabriat H (2005) Longitudinal thalamic diffusion changes after middle cerebral artery infarcts. J Neurol Neurosurg Psychiatry 76(2):200–205. doi:10.1136/jnnp.2004.041012
53. Yang Q, Tress BM, Barber PA, Desmond PM, Darby DG, Gerraty RP, Li T, Davis SM (1999) Serial study of apparent diffusion coefficient and anisotropy in patients with acute stroke. Stroke 30(11):2382–2390
54. Green HA, Pena A, Price CJ, Warburton EA, Pickard JD, Carpenter TA, Gillard JH (2002) Increased anisotropy in acute stroke: a possible explanation. Stroke 33(6):1517–1521
55. Mayer AR, Ling J, Mannell MV, Gasparovic C, Phillips JP, Doezema D, Reichard R, Yeo RA (2010) A prospective diffusion tensor imaging study in mild traumatic brain injury. Neurology 74(8):643–650. doi:10.1212/WNL.0b013e3181d0ccdd
56. Nael K, Trouard TP, Lafleur SR, Krupinski EA, Salamon N, Kidwell CS (2015) White matter ischemic changes in hyperacute ischemic stroke: voxel-based analysis using diffusion tensor imaging and MR perfusion. Stroke 46(2):413–418. doi:10.1161/STROKEAHA.114.007000
57. Zelaya F, Flood N, Chalk JB, Wang D, Doddrell DM, Strugnell W, Benson M, Ostergaard L, Semple J, Eagle S (1999) An evaluation of the time dependence of the anisotropy of the water diffusion tensor in acute human ischemia. Magn Reson Imaging 17(3):331–348
58. Alexander AL, Lee JE, Lazar M, Field AS (2007) Diffusion tensor imaging of the brain. Neurotherapeutics 4(3):316–329. doi:10.1016/j.nurt.2007.05.011
59. Carano RA, Li F, Irie K, Helmer KG, Silva MD, Fisher M, Sotak CH (2000) Multispectral analysis of the temporal evolution of cerebral ischemia in the rat brain. J Magn Reson Imaging 12(6):842–858
60. Liu Y, D'Arceuil HE, Westmoreland S, He J, Duggan M, Gonzalez RG, Pryor J, de Crespigny AJ (2007) Serial diffusion tensor MRI after transient and permanent cerebral ischemia in nonhuman primates. Stroke 38(1):138–145. doi:10.1161/01.STR.0000252127.07428.9c
61. Sotak CH (2002) The role of diffusion tensor imaging in the evaluation of ischemic brain injury—a review. NMR Biomed 15(7–8):561–569. doi:10.1002/nbm.786
62. Beaulieu C (2002) The basis of anisotropic water diffusion in the nervous system—a technical review. NMR Biomed 15(7–8):435–455. doi:10.1002/nbm.782
63. Sen PN, Basser PJ (2005) A model for diffusion in white matter in the brain. Biophys J 89(5):2927–2938. doi:10.1529/biophysj.105.063016
64. Stanisz G, Henkelman RM (2001) Effects of cellular swelling on diffusion in white matter. In: Proceedings of the 9th ISMRM, Glasgow, Scotland, p 350
65. Peled S (2007) New perspectives on the sources of white matter DTI signal. IEEE Trans Med Imaging 26(11):1448–1455
66. Douaud G, Jbabdi S, Behrens TE, Menke RA, Gass A, Monsch AU, Rao A, Whitcher B, Kindlmann G, Matthews PM, Smith S (2011) DTI measures in crossing-fibre areas: increased diffusion anisotropy reveals early white matter alteration in MCI and mild Alzheimer's disease. NeuroImage 55(3):880–890. doi:10.1016/j.neuroimage.2010.12.008
67. Pierpaoli C, Barnett A, Pajevic S, Chen R, Penix LR, Virta A, Basser P (2001) Water diffusion changes in Wallerian degeneration and their dependence on white matter architecture. NeuroImage 13(6 Pt 1):1174–1185. doi:10.1006/nimg.2001.0765
68. Teipel S, Ehlers I, Erbe A, Holzmann C, Lau E, Hauenstein K, Berger C (2014) Structural connectivity changes underlying altered working memory networks in mild cognitive impairment: a three-way image fusion analysis. J Neuroimaging. doi:10.1111/jon.12178
69. Adluru N, Destiche DJ, Lu SY, Doran ST, Birdsill AC, Melah KE, Okonkwo OC, Alexander AL, Dowling NM, Johnson SC, Sager MA, Bendlin BB (2014) White matter microstructure in late middle-age: effects of apolipoprotein E4 and parental family history of Alzheimer's disease. NeuroImage Clin 4:730–742. doi:10.1016/j.nicl.2014.04.008
70. Racine AM, Adluru N, Alexander AL, Christian BT, Okonkwo OC, Oh J, Cleary CA, Birdsill A, Hillmer AT, Murali D, Barnhart TE, Gallagher CL, Carlsson CM, Rowley HA, Dowling NM, Asthana S, Sager MA, Bendlin BB, Johnson SC (2014) Associations between white matter microstructure and amyloid burden in preclinical Alzheimer's disease: a multimodal imaging investigation. NeuroImage Clin 4:604–614. doi:10.1016/j.nicl.2014.02.001
71. Ryan NS, Keihaninejad S, Shakespeare TJ, Lehmann M, Crutch SJ, Malone IB, Thornton JS, Mancini L, Hyare H, Yousry T, Ridgway GR, Zhang H, Modat M, Alexander DC, Rossor MN, Ourselin S, Fox NC (2013) Magnetic resonance imaging evidence for presymptomatic change in thalamus and caudate in familial Alzheimer's disease. Brain 136(Pt 5):1399–1414. doi:10.1093/brain/awt065
72. Hasan KM, Halphen C, Boska MD, Narayana PA (2008) Diffusion tensor metrics, T2 relaxation, and volumetry of the naturally aging human caudate nuclei in healthy young and middle-aged adults: possible implications for the neurobiology of human brain aging and disease. Magn Reson Med 59(1):7–13. doi:10.1002/mrm.21434
73. Takenobu Y, Hayashi T, Moriwaki H, Nagatsuka K, Naritomi H, Fukuyama H (2014) Motor recovery and microstructural change in rubro-spinal tract in subcortical stroke. NeuroImage Clin 4:201–208. doi:10.1016/j.nicl.2013.12.003
74. Hope T, Westlye LT, Bjornerud A (2012) The effect of gradient sampling schemes on diffusion metrics derived from probabilistic analysis and tract-based spatial statistics. Magn Reson Imaging 30(3):402–412. doi:10.1016/j.mri.2011.11.003
75. Tensaouti F, Lahlou I, Clarisse P, Lotterie JA, Berry I (2011) Quantitative and reproducibility study of four tractography algorithms used in clinical routine. J Magn Reson Imaging 34(1):165–172. doi:10.1002/jmri.22584
76. Unrath A, Muller HP, Riecker A, Ludolph AC, Sperfeld AD, Kassubek J (2010) Whole brain-based analysis of regional white

matter tract alterations in rare motor neuron diseases by diffusion tensor imaging. Hum Brain Mapp 31(11):1727–1740. doi:10.1002/hbm.20971

77. Tuch DS, Reese TG, Wiegell MR, Makris N, Belliveau JW, Wedeen VJ (2002) High angular resolution diffusion imaging reveals intravoxel white matter fiber heterogeneity. Magn Reson Med 48(4):577–582. doi:10.1002/mrm.10268

78. Zhang H, Schneider T, Wheeler-Kingshott CA, Alexander DC (2012) NODDI: practical in vivo neurite orientation dispersion and density imaging of the human brain. NeuroImage 61(4):1000–1016. doi:10.1016/j.neuroimage.2012.03.072